

Microporous Hybrid Polymer with a Certain Crystallinity Built from Functionalized Cubic Siloxane Cages as a Singular Building Unit

Watcharop Chaikittisilp, Ayae Sugawara, Atsushi Shimojima, and Tatsuya Okubo*

*Department of Chemical System Engineering,
The University of Tokyo, 7-3-1 Hongo, Bunkyo-ku,
Tokyo 113-8656, Japan**Received June 27, 2010**Revised Manuscript Received August 10, 2010*

Ever-increasing demand for materials to be used in new technologies has accelerated the development of materials chemistry and engineering. Many potential marvelous applications can be envisaged for ordered nanoporous materials, particularly in the fields of adsorption, catalysis, separation, and electronics.^{1,2} Among nanoporous materials practically used in the chemical industry, zeolites show great performance in molecular discrimination through their ion-exchanging and molecular-sieving capabilities. Discoveries of new zeolitic frameworks, however, have mainly relied upon (pseudo)serendipity and Edisonian trial-and-error approach.³ Designed synthesis of zeolites with tailored pore structures is still impossible, probably because of a lack of understanding in their formation mechanisms.^{3,4} This limits their uses in emerging applications needing more finely designed architectures.

The stepwise increase in the structural order and dimension of the frameworks in bottom-up fashion has been considered as one of the strategies to achieve well-designed nanoporous materials with desired structures and functions.^{5,6} Structure-directing assembly of strategic molecular building units into the extended frameworks has been applied to design and synthesize metal–organic and covalent organic frameworks (MOFs and COFs).^{7,8} However, most MOFs synthesized thus far suffer from relatively low thermal and hydrothermal stabilities, whereas crystalline COFs have to be synthesized in strictly reversible process under thermodynamic control.

Alternatively, porous covalent organic polymers have been synthesized by many common organic reactions.^{9–15} Such polymers are constructed solely by covalent links between light elements; accordingly, they feature relatively high thermal stability and low density. An approach toward the development of organic microporous materials with well-defined pores is based on the idea of mimicking the architecture of inorganic zeolites, MOFs, and COFs.^{11,12a} A series of microporous (conjugated) polymer networks has been synthesized using several cross-coupling reactions.^{11–15} In addition, recent works have revealed that pore size distributions of some organic polymers are narrow and can be tuned by simply varying the length of the rigid organic linkers.^{11,13} In contrast to COFs, such organic polymers are formed under kinetic control and irreversible reaction; hence, polymers with highly porous and long-range order are hardly obtained.

Very recently, we reported the synthesis of inorganic–organic hybrid microporous materials by directly linking functionalized cubic octameric siloxane cages (Si₈O₁₂), commonly known as double four-ring (D4R), with rigid organic linkers.¹¹ The resulting hybrid materials possess relatively high surface areas and comparable thermal stability. On the basis of the pore size distribution, the local networks of the hybrids have been implied to be interpenetration or catenation-like structures. Usually, such interpenetration is observed in crystalline solids and polymeric materials when the length of strut or ligand is too long.¹⁶ This phenomenon could broaden the pore size distribution, especially in the case of porous macromolecular networks. Connecting the nodes with the sterically bulky or short linkers can prevent such interpenetration.^{16a}

*Corresponding author. E-mail: okubo@chemsys.t.u-tokyo.ac.jp.

- (1) Davis, M. E. *Nature* **2002**, *417*, 813.
- (2) Fujita, S.; Inagaki, S. *Chem. Mater.* **2008**, *20*, 891.
- (3) (a) Davis, M. E.; Lobo, R. F. *Chem. Mater.* **1992**, *4*, 756. (b) Corma, A.; Davis, M. E. *ChemPhysChem* **2004**, *5*, 304.
- (4) (a) Wakihara, T.; Okubo, T. *Chem. Lett.* **2005**, *34*, 276. (b) Burton, A. W. *J. Am. Chem. Soc.* **2007**, *129*, 7627.
- (5) (a) Ozin, G. A. *Adv. Mater.* **1992**, *4*, 612. (b) Morris, R. E. *J. Mater. Chem.* **2005**, *15*, 931.
- (6) Moteki, T.; Chaikittisilp, W.; Shimojima, A.; Okubo, T. *J. Am. Chem. Soc.* **2008**, *130*, 15780.
- (7) (a) Eddaoudi, M.; Moler, D. B.; Li, H.; Chen, B.; Reineke, T. M.; O'Keeffe, M.; Yaghi, O. M. *Acc. Chem. Res.* **2001**, *34*, 319. (b) Kitagawa, S.; Kitaura, R.; Noro, S.-I. *Angew. Chem., Int. Ed.* **2004**, *43*, 2334.
- (8) El-Kaderi, H. M.; Hunt, J. R.; Mendoza-Cortés, J. L.; Côté, A. P.; Taylor, R. E.; O'Keeffe, M.; Yaghi, O. M. *Science* **2007**, *316*, 268.

- (9) McKeown, N. B.; Budd, P. M.; Msayib, K. J.; Ghanem, B. S.; Kingston, H. J.; Tattershall, C. E.; Makhseed, S.; Reynolds, K. J.; Fritsch, D. *Chem.—Eur. J.* **2005**, *11*, 2610.
- (10) (a) Germain, J.; Hradil, J.; Fréchet, J. M. J.; Svec, F. *Chem. Mater.* **2006**, *18*, 4430. (b) Wood, C. D.; Tan, B.; Trewin, A.; Niu, H.; Bradshaw, D.; Rosseinsky, M. J.; Khimiyak, Y. Z.; Campbell, N. L.; Kirk, R.; Stöckel, E.; Cooper, A. I. *Chem. Mater.* **2007**, *19*, 2034.
- (11) Chaikittisilp, W.; Sugawara, A.; Shimojima, A.; Okubo, T. *Chem.—Eur. J.* **2010**, *16*, 6006.
- (12) (a) Ben, T.; Ren, H.; Ma, S.; Cao, D.; Lan, J.; Jing, X.; Wang, W.; Xu, J.; Deng, F.; Simmons, J. M.; Qiu, S.; Zhu, G. *Angew. Chem., Int. Ed.* **2009**, *48*, 9457. (b) Schmidt, J.; Werner, M.; Thomas, A. *Macromolecules* **2009**, *42*, 4426.
- (13) (a) Jiang, J.-X.; Su, F.; Trewin, A.; Wood, C. D.; Campbell, N. L.; Niu, H.; Dickinson, C.; Ganin, A. Y.; Rosseinsky, M. J.; Khimiyak, Y. Z.; Cooper, A. I. *Angew. Chem., Int. Ed.* **2007**, *46*, 8574. (b) Jiang, J.-X.; Su, F.; Trewin, A.; Wood, C. D.; Niu, H.; Jones, J. T. A.; Khimiyak, Y. Z.; Cooper, A. I. *J. Am. Chem. Soc.* **2008**, *130*, 7710.
- (14) (a) Weber, J.; Thomas, A. *J. Am. Chem. Soc.* **2008**, *130*, 6334. (b) Kuhn, P.; Forget, A.; Su, D.; Thomas, A.; Antonietti, M. *J. Am. Chem. Soc.* **2008**, *130*, 13333.
- (15) Farha, O. K.; Spokoyny, A. M.; Hauser, B. G.; Bae, Y.-S.; Brown, S. E.; Snurr, R. Q.; Mirkin, C. A.; Hupp, J. T. *Chem. Mater.* **2009**, *21*, 3033.
- (16) (a) Farha, O. K.; Malliakas, C. D.; Kanatzidis, M. G.; Hupp, J. T. *J. Am. Chem. Soc.* **2010**, *132*, 950. (b) Klempner, D. *Angew. Chem., Int. Ed.* **1978**, *17*, 97.

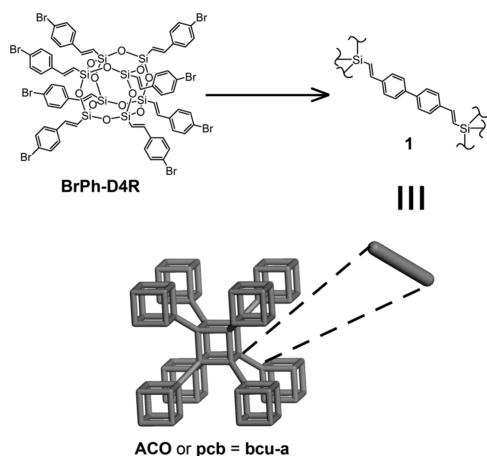


Figure 1. Schematic design of the hybrid polymer **1** built by Ni⁰-mediated Yamamoto polymerization of the **BrPh-D4R** cages.

We report herein self-polymerization of bromophenylethynyl-terminated cubic D4R siloxane cages (**BrPh-D4R**) by nickel(0)-mediated Yamamoto reaction¹² (see Figure 1). We have expected that, as a result of the shortened linkers, the obtained polymer **1** would exhibit less pronounced interpenetration, and thereby more uniform pore size distribution and higher structural periodicity.

As D4R cages are very rigid, connecting the D4R units through two-coordinated linear linkers would result in the ACO topology (**pcb** or **bcu-a** nets) as a default structure.¹⁷ Such linear ditopic linkers can be formed simultaneously by homocoupling of **BrPh-D4R**, synthesized by the reported procedure,¹¹ in the presence of the stoichiometric amounts of bis(1,5-cyclooctadiene)nickel(0), 2,2'-bipyridyl, and 1,5-cyclooctadiene. The hybrid polymer **1** was then recovered, successively washed with several solvents, and dried in vacuo (see details in the Supporting Information).

The completion of the reaction was confirmed by energy-dispersive X-ray fluorescence spectrometry. No bromine end groups were detected (the average Br/Si < 0.001), indicating that nearly all end groups have been reacted. The product yield was higher than 95%. Also, the average Ni/Si molar ratio was less than 0.006, suggesting that although the stoichiometric amount of nickel complex is needed for the reaction, the procedures employed were effective to remove it from the desired product. Success in the polymerization was also confirmed by solid-state ¹H-¹³C CP/MAS NMR spectroscopy (see Figure S1 in the Supporting Information). The signal arising from carbons at biphenyl bridge is observed at $\delta = 141.5$ ppm, proving the homocoupling of the **BrPh-D4R** molecules. The spectrum displays the strong signal at $\delta = 127$ ppm, which can be assigned to unsubstituted phenylene carbon atoms. The additional resonances observed at $\delta = 137, 118,$ and 149 ppm are attributed to the other substituted phenylene carbon and two ethylene carbon atoms, respectively.

Further investigation on the local structure of the hybrid polymer **1** was performed by solid-state ²⁹Si MAS NMR. The spectrum shown in Figure 2a displays

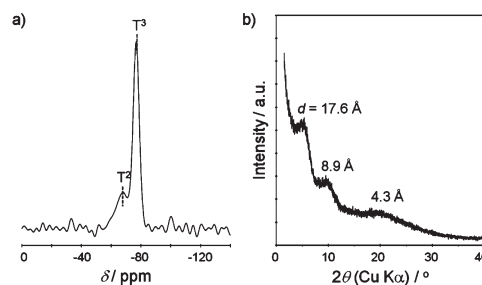


Figure 2. (a) ²⁹Si MAS NMR spectrum and (b) powder XRD pattern of the hybrid polymer **1**.

the predominant signal at $\delta = -76.8$ ppm with a small shoulder at $\delta = \text{ca. } -68$ ppm, assigned to T³ and T² silicon units, respectively (Tⁿ: CSi(OSi)_n(OH)_{3-n}). The degree of siloxane bond (Si-O-Si) cleavage was calculated to be 5.9%, indicating that only a small part of the D4R cages was collapsed during the polymerization. Previous reports on D4R-based materials claimed that D4R units were statistically retained in the porous networks.^{11,18,19} Based on this small portion of the cleaved siloxane bonds, it is unambiguous that D4R cages exist in the final hybrid **1**. The existence of the D4R cages offers the opportunities for postfunctionalization of the networks by several means, as the D4R cages can trap very small species such as atomic hydrogen and fluoride ion.²⁰ Also, one can expect that connection of the truly retained D4R cages with straight and rigid linkers would provide the orderly microscopic arrangement of the cages and subsequently the narrow micropore size distribution.

Powder XRD pattern of the hybrid **1** shown in Figure 2b indicates that the obtained hybrid is not fully crystalline. However, in contrast to the typical amorphous porous polymers,^{9-15,18,19} the XRD pattern shows three broad peaks centered at $2\theta = 5.0, 10.0,$ and 20.7° , equivalent to *d*-spacing distances of 17.6, 8.9, and 4.3 Å, respectively. This can imply that the obtained hybrid possesses (locally) molecular homogeneity and long-range order although the degree of the order is not very high. A few reported D4R-based materials with a certain structural periodicity have shown the XRD peak at low scattering angles corresponding to $d = \text{ca. } 10$ Å.¹⁹ Hagiwara et al. reasoned that this structural periodicity is not directly associated with the D4R units, but they may be attributed to some siloxane ring structures, especially tetrameric siloxane four-ring.^{19a} To the best of our knowledge, however, the hybrid **1** is the first D4R-based polymer network exhibiting the XRD peak equivalent to such *d*-spacing as large as 17.6 Å obtained in the absence

(17) Delgado-Friedrichs, O.; O'Keeffe, M.; Yaghi, O. M. *Phys. Chem. Chem. Phys.* **2007**, *9*, 1035.

(18) (a) Shimojima, A.; Goto, R.; Atsumi, N.; Kuroda, K. *Chem.—Eur. J.* **2008**, *14*, 8500. (b) Zhang, L.; Abbenhuis, H. C. L.; Yang, Q.; Wang, Y.-M.; Magusin, P. C. M. M.; Mezari, B.; van Santen, R. A.; Li, C. *Angew. Chem., Int. Ed.* **2007**, *46*, 5003.

(19) (a) Hagiwara, Y.; Shimojima, A.; Kuroda, K. *Chem. Mater.* **2008**, *20*, 1147. (b) Hagiwara, Y.; Shimojima, A.; Kuroda, K. *Bull. Chem. Soc. Jpn.* **2010**, *83*, 424. (c) Auner, N.; Bats, J. W.; Katsoulis, D. E.; Suto, M.; Tecklenburg, R. E.; Zank, G. A. *Chem. Mater.* **2000**, *12*, 3402.

(20) (a) Sasamori, R.; Okaue, Y.; Isobe, T.; Matsuda, Y. *Science* **1994**, *265*, 1691. (b) Anderson, S. E.; Bodzin, D. J.; Haddad, T. S.; Boatz, J. A.; Mabry, J. M.; Mitchell, C.; Bowers, M. T. *Chem. Mater.* **2008**, *20*, 4299.

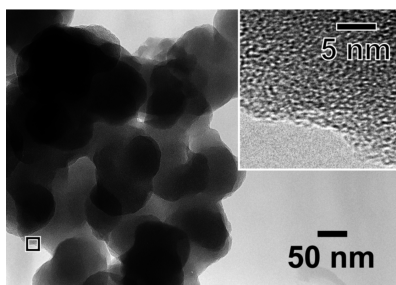


Figure 3. High-resolution TEM image of the hybrid polymer **1**. Inset shows the magnified image of the marked area.

of any templates. This XRD peak is likely attributed to the periodic arrangement of the D4R cages linked by ethylenephylene bridges. Indeed, the strong peaks at $2\theta = 5.0$ and 10.0° would arise from (110) and (220) planes, respectively, as a lattice parameter of the model constructed based on ACO topology is about 25 \AA (see Figure S2 in the Supporting Information).

Size and morphology of the polymeric particles were observed by a field-emission scanning electron microscope (FE-SEM). The hybrid polymer **1** shows a round shape with the size of $100\text{--}300 \text{ nm}$ (see Figure S3 in the Supporting Information). Investigation by a transmission electron microscope (TEM) reveals that the particles have micropores with relatively uniform diameters (Figure 3). Note that hybrid **1** was very stable under the electron beam.

The porous character of the obtained hybrid was studied by nitrogen adsorption. As shown in Figure 4a, the isotherm shows a steep increase in adsorbed volume at low relative pressure and gradual increases at higher relative pressure, suggesting that the hybrid **1** is a microporous material. The apparent specific Brunauer–Emmett–Teller (BET) surface area and the total pore volume (at $P/P_0 = 0.99$) of the network were calculated to be $1045 \pm 60 \text{ m}^2 \text{ g}^{-1}$ and $1.01 \pm 0.02 \text{ cm}^3 \text{ g}^{-1}$, respectively, averaged from two different samples synthesized from different batches where each sample was measured twice. The non-local density functional theory (NL-DFT) method was employed to evaluate pore size distribution as shown in Figure 4b. Bimodal pore diameters of about 7.0 and 11.6 \AA are observed. The narrow and sharp distribution at the diameter of 11.6 \AA indicates that the material predominantly contains micropores with this size. The calculated pore diameter is also consistent with the model (see Figure S2 in the Supporting Information), in which the largest free space along [100] direction is about 10.5 \AA . The smaller pore diameter of 7 \AA might correspond to the smaller space along [111] direction (see Figure S2d in the Supporting Information) and/or catenation-like networks. The XRD and the nitrogen adsorption results suggest that the hybrid **1** possesses preferential long-range orders with local ACO topology. Also, catenation or interpenetration of the framework found in the similar networks reported previously¹¹ can be suppressed by shortening the length of the linkers between D4R cages.

The hydrogen adsorption capacity of the hybrid **1** was also evaluated (see Figure S4 in the Supporting Information). The hydrogen uptake at 77 K and 760 Torr

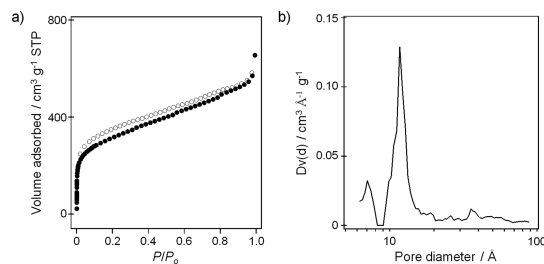


Figure 4. (a) Nitrogen adsorption–desorption isotherm (filled and empty symbols represent adsorption and desorption branches, respectively) and (b) NL-DFT pore size distribution of the hybrid polymer **1**.

and the isosteric heat of adsorption at low hydrogen coverage are $0.82 \text{ wt } \%$ and 7.2 kJ mol^{-1} , respectively. Both adsorption capacity and isosteric heat of adsorption of the hybrid **1** are comparable to those of several good candidates as media for hydrogen storage, including porous organic polymers and metal organic frameworks.^{9–11}

To obtain information on the thermal stability of the hybrid **1**, thermogravimetric and differential thermal analyses (TG-DTA) in the presence and absence of gaseous oxygen were performed (see Figure S5 in the Supporting Information). In the $10\% \text{ O}_2/90\% \text{ He}$ atmosphere, the obtained hybrid **1** is stable up to around $390 \text{ }^\circ\text{C}$, which is slightly more stable than the D4R-based porous hybrid reported previously,¹¹ the thermal stability of the hybrid **1** is comparable to other porous organic polymers.^{9–15} In the presence of oxygen, a slight increase in TG weight starting at ca. $310 \text{ }^\circ\text{C}$ is observed, whereas no increase in TG weight is noticeable in the pure He atmosphere. Thus, this increase in TG weight is likely because of the oxidation of the resulting hybrid, particularly the unsaturated ethylene carbon–carbon bonds.

In summary, a microporous inorganic–organic hybrid material has been synthesized simply by self-linking of the BrPh-D4R cages as singular building units via Yamamoto polymerization. The resulting hybrid exhibits relatively high surface area and pore volume, and comparably high thermal stability. Importantly, most of the D4R cages are retained in the resulting network. In comparison with the previous report,¹¹ the present study demonstrates that interpenetration of the polymer network can be less pronounced by decreasing the linker distances, as evidenced by very narrow pore size distribution. Unprecedentedly, this D4R-based hybrid shows a certain degree of crystallinity. Improvement in its degree of the order is underway.

Acknowledgment. Partial financial supports by a Grant-in-Aid for Scientific Research (B), JSPS, and by Global COE program (Mechanical Systems Innovation), MEXT, Japan are acknowledged. A part of this work was conducted in Center for Nano Lithography & Analysis, The University of Tokyo, supported by MEXT, Japan. We thank Mr. T. Moteki and Mr. M. Kubo for their technical assistance.

Supporting Information Available: Experimental details; ^1H – ^{13}C CP/MAS NMR spectrum, TG-DTA results, FE-SEM image, molecular models, and H_2 adsorption results of the resulting hybrid (PDF). This material is available free of charge via the Internet at <http://pubs.acs.org>.